

# Electrochemical and Spectroscopic Studies of Arylazo-2-naphthol Metal Complexes in Dimethylformamide Solution

Rafik O. Loutfy\* and James H. Sharp

Contribution from the Xerox Research Centre of Canada Ltd., Mississauga, Ontario L5L 1J9, Canada. Received November 8, 1976

**Abstract:** The molecular properties of the sodium and those of the calcium, strontium, barium, and magnesium salts of the azo pigment, 2'-naphthylazo-6-bromo-2-naphthol (NABN)-1'-sulfonate, were determined and compared using polarographic, voltammetric, and spectroscopic techniques. It was found that the sodium salt has a tendency to form high molecular weight linear aggregates in dimethylformamide. The driving force appears to be intermolecular hydrogen bonding. Utilizing a number of electrochemical techniques it was possible to develop an analytical procedure to determine the stoichiometry of the azo pigment to metal ion and to explore the molecular aggregation of azo pigments in solution. Polarographic and potentiometric titration measurements indicated that alkaline earth metal ions displace both the phenolic hydrogen and the sulfonic sodium ions to form stable six-membered intramolecular complexes. In contrast to the sodium salt, these azo pigment metal complexes showed a definite tendency toward the formation of parallel plane dimers in DMF. The equilibrium association constants were found to be related to the electronegativity of the metal ions.

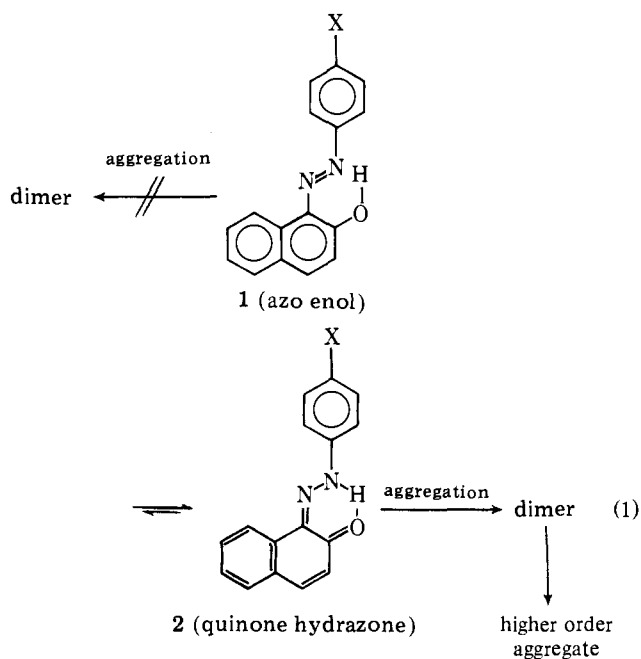
Azo molecules comprise the largest single class of organic materials from which varying colors of dyes and pigments can be derived. Such compounds have found many applications such as the dyeing of fabric, the coloring of toners, and as dyes or photosensitive species in photographic or electrophotographic systems. The semiconducting and photoconducting properties of organic azo materials have also received increasing attention<sup>1</sup> because of their potential to replace inorganic semiconductors and photoconductors.

Dyes and pigments are notoriously known to associate in solutions. The physical pigment-pigment interactions are of importance both at the theoretical level because of the thermodynamic considerations and at the practical level where such interactions may be advantageous or disadvantageous with regard to spectral response and sensitivity of the pigments. The aggregation of dyes has been studied extensively in aqueous solution through a number of experimental approaches, e.g., absorption spectra,<sup>2</sup> electrical conductivity,<sup>3</sup> light scattering,<sup>4</sup> sedimentation,<sup>5</sup> and more recently by polarography.<sup>6</sup> The merits of the various techniques are described at length elsewhere.<sup>7-9</sup> However, all these methods were applied to highly purified, water-soluble dyes. Our interest lies in the metal salts of arylazo-2-naphthol pigments which are highly intractable, insoluble materials in most common solvents.

An important feature of substituted arylazo-2-naphthols is that they participate in a quinone hydrazone  $\rightleftharpoons$  azo enol tautomeric equilibrium (eq 1).<sup>10,11</sup>

It was demonstrated by NMR, visible absorption, and Raman spectroscopy<sup>10,11</sup> that only the quinone hydrazone tautomer participates in the process of molecular aggregation. The azo enol tautomer is relatively inactive toward the formation of molecular aggregates.<sup>12</sup> In addition, the electronic transition of crystalline arylazo-2-naphthol compounds is strongly red shifted (1000 Å) relative to that for the dissolved or amorphous solid species. This large spectral shift was attributed to intermolecular hydrogen-bonded aggregates, whose electronic structures are very closely approximated by that of the protonated azo compound.<sup>12</sup> Apparently, the most important driving force for tautomerization, aggregation, and spectral changes of the previously studied arylazo-2-naphthols is due to inter- and intramolecular hydrogen bonding.

The electrochemical behavior of azo dyes and their metal complexes has been extensively studied using polarographic techniques in aqueous solution.<sup>13-16</sup> The polarographic re-

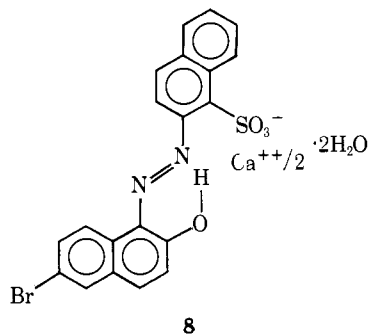


duction of these compounds appears to be the only case in which the organometallic complex yields a wave distinctly different from that of the organic dyes. In aqueous solution this reduction is seen as a single four-electron wave producing the corresponding amines.

On the other hand, polarography of azo compounds in nonaqueous solvents has been less thoroughly studied,<sup>13</sup> and studies of their metal complexes are almost nonexistent. Bard and Sadler have shown<sup>17</sup> that for a series of aromatic azo compounds in dimethylformamide (DMF) solution the reduction occurs in two one-electron steps. The product of the first electron transfer is a stable anion radical, while the dianion formed by the second electron transfer undergoes further chemical reaction. Kuder et al.<sup>1</sup> recently described the polarographic reduction and oxidation of a series of substituted derivatives of 1-phenylazo-2-naphthols in acetonitrile solution. Similarly, it was found that both reduction and oxidation proceed by reversible one-electron transfer processes.

An objective of the present paper is to determine the influence of various metal ions on the molecular aggregation, molecular structure, electronic absorption, and the molecular

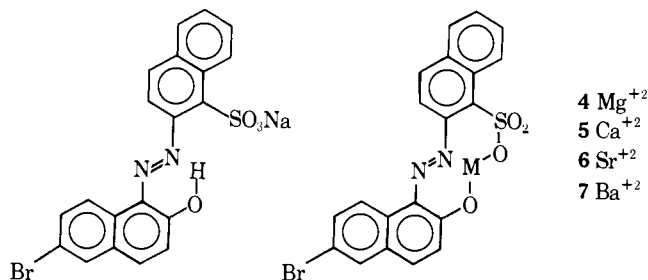
Table I. Calculated and Analyzed Elemental Analysis for 8



	C	H	N	Br	S
Calcd for C <sub>40</sub> H <sub>24</sub> Br <sub>2</sub> CaN <sub>4</sub> O <sub>8</sub> S <sub>2</sub>	50.4	2.54	5.88	16.77	6.73
Calcd for C <sub>40</sub> H <sub>24</sub> Br <sub>2</sub> CaN <sub>4</sub> O <sub>8</sub> S <sub>2</sub> ·2H <sub>2</sub> O	48.58	2.83	5.67	16.20	6.48
Found	47.71	2.29	5.49	16.58	6.33

energy levels of arylazo-2-naphthol complexes. Electrochemical and spectroscopic techniques are employed for this purpose.

The molecular structures of the compounds studied in this investigation are given below.



The polarographic reduction of these compounds in DMF solution at DME will be described first and then a relationship between diffusion current and concentration will be developed to gain an understanding of aggregation phenomena. Additional support for aggregate structures is gained through spectroscopic studies. Electrochemical redox potentials are utilized to formulate a description of the electronic solid state energy level structure of the aggregate systems.

## Experimental Section

**1. Synthesis of Sodium Salt.** A sample of sodium 1'-sulfo-2'-naphthylazo-6-bromo-2-naphthol (**3**) was synthesized by diazotization of 2-aminonaphthalene-1-sulfonic acid followed by coupling of the diazonium salt with 6-bromo-2-naphthol in aqueous alkaline solution to give the sodium salt in 90% yield. Other metal ion derivatives were synthesized from the parent compound **3**, by displacing the sodium ions in DMF solution using the appropriate metal chloride.

Spectrograde *N,N'*-dimethylformamide (DMF) was passed through a column of activated alumina immediately before use. Tetraethylammonium perchlorate (TEAP) (Eastman Kodak) was crystallized from water and vacuum dried at 100 °C for 6 h. Anhydrous calcium, magnesium, strontium, and barium chlorides were all Fisher analytical grade. The salts were dried in a vacuum oven at 160 °C overnight. These salts are all soluble in DMF except BaCl<sub>2</sub>, which is only slightly soluble.

**2. Synthesis and Analysis of Metal Salts of NABN Sulfonate.** The sodium salt of NABN sulfonate, **3** (1.0 g) was dissolved in 500 mL of warm DMF. To the well-stirred solution 50 mL of DMF containing 0.5 g of calcium chloride was added. The temperature was raised and maintained at 100 °C for 30 min. Two different calcium salts were obtained depending on the method of precipitation. Aqueous precipitation of the DMF solution led to the formation of a brick red powder, **8**. Analysis of a nitric acid solution of **8** using atomic absorption in-

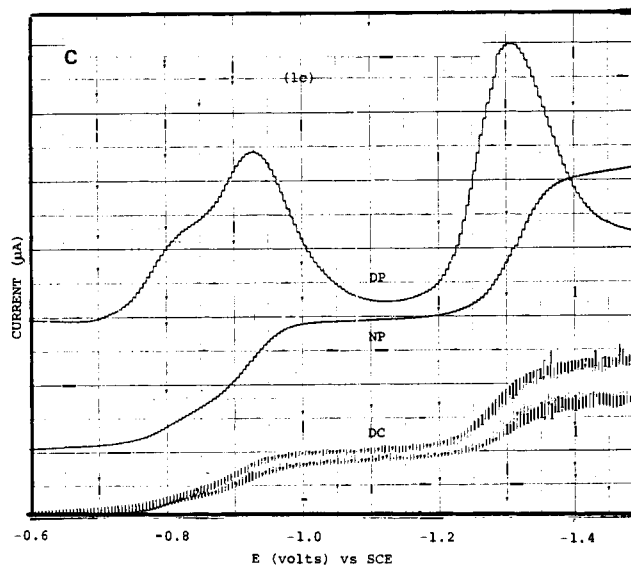
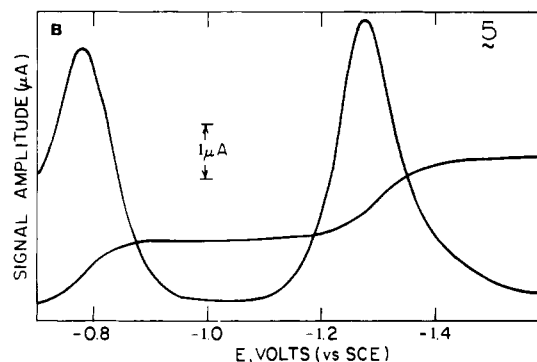
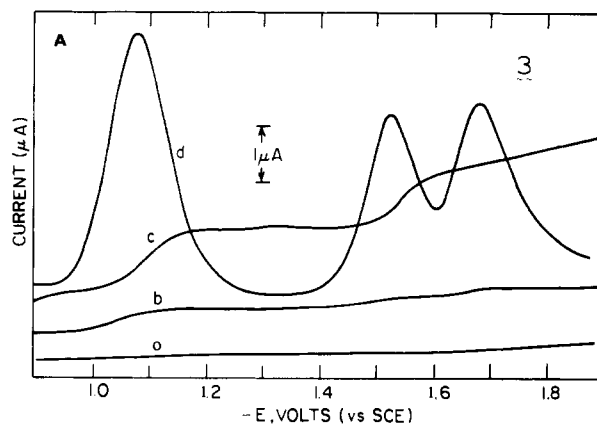


**Figure 1.** The reduction of **3** (A) and **5** (B). The solution was 0.3 mM of the azo pigment in DMF containing 0.1 M TEAP, (a) background current; (b) dc; (c) normal pulse (NP) and (d) differential pulse (DP). (C) The reduction of NABNS-magnesium complex in DMF

indicated the presence of 4.03% calcium which is consistent with a structure of one calcium ion per two azo pigment molecules. This was confirmed by elemental analysis as shown in Table I.

On the other hand, nonaqueous (benzene) precipitation off the DMF solution led to a purplish-red solid, **5**. According to atomic absorption analysis, the 1:1 complexes for the Ca, Sr, and Ba all resulted when nonaqueous precipitation was employed. Unlike these alkaline earth metal salts of NABN sulfonate pigments, which form the 1:1 complex in DMF, the magnesium salt forms a 1:2 molecular structure preferentially. This conclusion is based both on polarographic and atomic absorption analysis.

**3. Electrochemical Measurements. a. Dc and Pulse Polarograms.** These were measured with a three-electrode polarograph, PAR 174. The solutions employed were 0.3 mM depolarizer and 0.1 M TEAP

Table II. Electrochemical Reduction Half-Wave Potentials Data for Metal-1'-sulfo-2'-naphthylazo-6-bromo-2-naphthol<sup>a</sup>

No.	Metal ion	Polarographic reduction potential data					
		First reduction wave			Second reduction wave		
		$-E_{1/2}^{\text{red}} \text{ (I)}^b$	$I_d^c$	$-\text{Slope}^d$	$-E_{1/2}^{\text{red}} \text{ (II)}$	$I_d$	$-\text{Slope}$
3	Sodium	1.09	3.23	0.06	1.54	2.5	0.043
4	Magnesium	0.80; 0.92	5.12	0.07	1.31 (1.41) <sup>e</sup>	7.0	0.062
5	Calcium	0.79	2.79	0.06	1.30	3.81	0.094
6	Strontium	0.88	2.84	0.073	1.36 (1.42)	2.60	0.10
7	Barium	0.90	2.77	0.078	1.38 (1.45)	2.31	0.10

<sup>a</sup> The solution was 0.10 M TEAP in DMF. <sup>b</sup> Potentials are in volts vs. an aqueous saturated calomel electrode (SCE). <sup>c</sup>  $I_d = i_d/m^{2/3}t^{1/6}C_R$ , Lingane's constant, where  $i_d$  is the diffusion current,  $m$  is the mercury flow rate in mg/s,  $t$  is the mercury drop time, and  $C_R$  is the concentration of the electroactive species in millimoles (0.29). <sup>d</sup> Slope of plot of  $E_{1/2}$  vs.  $\log i/(i_d - i)$  in volts. <sup>e</sup> Values in parentheses are the potential of third wave or maxima.

in DMF. The cell electrode consists of a dropping mercury working electrode, a platinum wire auxiliary electrode, and an aqueous saturated potassium chloride calomel reference electrode (SCE) with a nonaqueous salt bridge. The capillary characteristics of the DME (at open circuit) follow: flow rate,  $m$ , 1.146 mg Hg/s and drop time,  $t$ , 6.8 s at a height,  $h$ , 70 cm in DMF. Measurements were performed at room temperature (22 °C) under a dried argon atmosphere. For oxidation, a stationary platinum disk (Beckman) served as the working electrode. The voltammograms are not corrected for uncompensated resistance.

**b. Potentiometric Titration Measurements.** It is known that the single polarographic wave of azo dyes splits into two reduction waves in the presence of trace metal ions.<sup>18</sup> This technique has been extensively used to polarographically determine metal ions in aqueous solutions. This same principle was utilized to determine the stoichiometry of the azo pigment to the metal ion in nonaqueous DMF. This method is quantitative since the height of the new wave is usually proportional to the metal ion concentration and shifted from the first. The sodium salt **3** was used as the parent material, from which a stock solution of 0.29 mM in DMF containing 0.1 M TEAP was prepared. This solution exhibited a well-defined polarographic reduction wave potential (−1.09 V), as shown in Figure 1.

**c. Aggregate Determination.** McKay and Hilson<sup>6</sup> have recently developed a polarographic method for determining the aggregation number of dyes in the presence of an electrolyte in aqueous solution. In this work the method has been extended to study the aggregation of the metal azo pigments in nonaqueous aprotic media (DMF). A stock solution of each of the compounds **3–7** was prepared in DMF ( $10^{-2}$  M), heated to 80 °C for 2 h, and then placed in a dark place overnight. A known aliquot of the stock solution was added to 25 mL of DMF solution containing 0.1 M TEAP electrolyte. The mixture was degassed for 15 min with purified argon gas, and polarographic measurements were then carried out. This process was repeated for the azo pigment–metal complex concentration range from  $10^{-5}$  to  $10^{-3}$  M. The diffusion current,  $i_d$ , electroactive concentration,  $C_R$ , and the electrode capillary characteristics for compound **3** and **5** are given in Tables IV and V.

**4. Spectroscopic Measurements.** The change in absorption spectra of pigments **3–7** in DMF as a function of concentration has also been determined to independently obtain the respective association constants. Solution spectra of **3–7** were determined using solutions of ca.  $1-2 \times 10^{-5}$  M in DMF (spectral grade).

For each pigment, four solutions were prepared in the  $10^{-5}$ – $10^{-3}$  M concentration range. Spectra were run on a Cary 17 spectrophotometer using 0.01, 0.1, 1, and 5 cm matched quartz cells. The concentration dependence of the absorption spectra of pigments **3–5** is shown in Figures 5–7. Those of pigment **6** and **7** are similar to that of pigment **5**.

## Results

**1. Polarographic Methods.** The polarographic reduction of each of the metal complexes of 1'-sulfo-2'-naphthylazo-6-bromo-2-naphthol shows at least two well-defined waves. The

polarogram given in Figure 1, that of the sodium NABN sulfonate, **3**, could be considered typical of the polarographic behavior exhibited by every member of the series, except that in most other cases the third reduction wave is less well defined and merges with the second wave. The half-wave reduction potential,  $E_{1/2}$ , and other polarographic data are given in Table II. The slope of the plot of  $E$  vs.  $\log [i/(i_d - i)]$  for the first reduction wave ranges from 0.06 to 0.078 V, suggesting a reversible, one-electron reaction. A similar plot for the second wave of each of these compounds shows slopes ranging from 0.043 for the sodium azo pigment to 0.10 V for the strontium and barium azo pigments. The diffusion currents of the first reduction wave varied as the square root of the height of the mercury column (corrected for Hg back pressure). These results indicate that the limiting current is diffusion limited. It was also found that the polarographic reduction potential was constant over the concentration range  $10^{-5}$ – $10^{-2}$  M. However, over the same concentration range the limiting current was not proportional to concentration, i.e.,  $i/C \neq \text{constant}$ . This point will be discussed in detail later. For the purpose of this study we will focus only on the first reduction wave of these compounds. The polarographic behavior of this series of organic azo metal complexes in DMF at DME is, in general, very similar to those observed for azobenzene, azonaphthalene,<sup>17</sup> and azo-2-naphthols<sup>1</sup> in aprotic solvent.

**2. Voltammetric Methods.** The voltammetric oxidation of each of the members of this series showed an irreversible one-electron reaction at the platinum disk electrode. Values are given in Table III. The voltammograms shown in Figure 2 for compound **3** are typical of the voltammetric behavior exhibited by every member of the series. No cathodic peak was observed upon scan reversal following the oxidation step. The peak potential shifts anodically about 30 mV for a tenfold increase in scan rate which characterizes the behavior exhibited by reversible charge transfer followed by a very fast chemical reaction. Some interference from the excess chloride ions was observed in the case of the Ba-azo complex since the oxidation of  $\text{Cl}^-$  occurs at  $\sim 1.3$  V vs. SCE.

**3. Potentiometric Titration Measurements.** Typical potentiometric titration polarograms are given in Figure 3 for the strontium complex. The height of the displaced wave reached a constant maximum value at a metal ion concentration equivalent to that required to form a 1:1 complex. Similar results were obtained for every member of the series. Figure 4 shows a plot of the limiting reduction current of both the original sodium azo pigment and the formed metal complex vs. the metal ion concentration, where  $i_{\text{Na-azo}}$  reaches zero at a metal ion concentration equivalent to the initial concentration

Table III. Voltammetric Oxidation Half-Wave Potential of NABN Sulfonate and Its Metal Complexes

No.	Metal ion	Voltammetric oxidation potential data first oxidation wave				
		$E_p^b$	$E_{p1/2}$	Slope <sup>c</sup>	$E_{1/2}^{ox}$	$\beta^d$
3	Sodium	1.15	1.08	0.07	1.05	0.68
4	Magnesium	1.08	0.98	0.076	0.98	0.60
5	Calcium	1.08	0.97	0.073	0.97	0.60
6	Strontium	1.05	0.95	0.072	0.95	0.60
7	Barium	1.01	0.93	0.08	0.93	0.60

<sup>a</sup> Planar platinum disk electrode, the solution 0.1 M TEAP in DMF. <sup>b</sup> In volts vs. SCE. <sup>c</sup> Slope of plot of  $E$  vs.  $\log i/(i_d - i)$ . <sup>d</sup> Electron transfer coefficient.

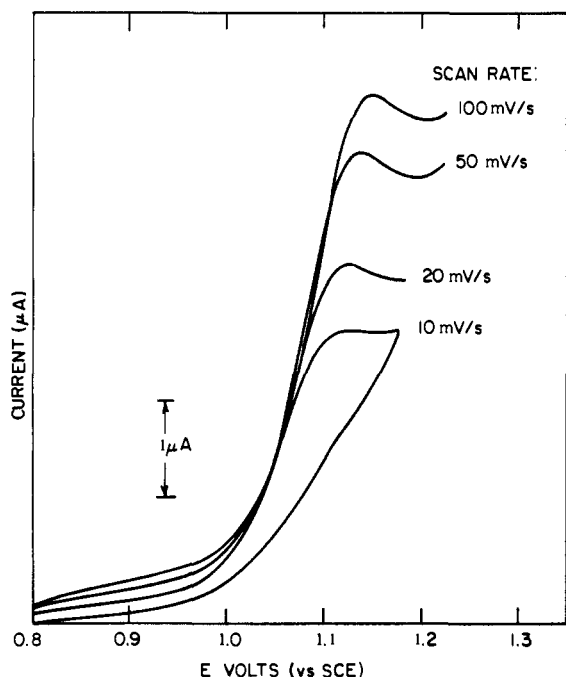
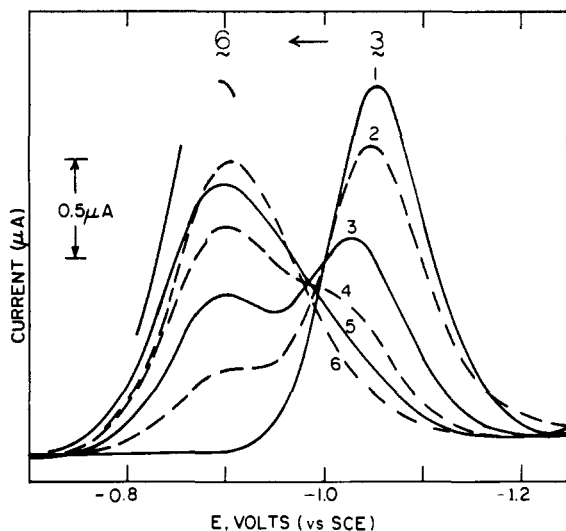
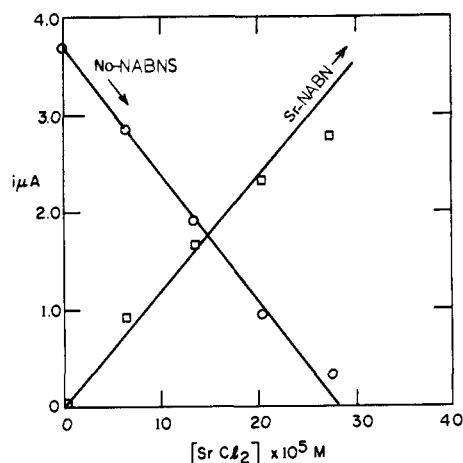


Figure 2. Voltammogram of 3 in DMF containing 0.1 M TEAP at pde.

Figure 3. Typical differential pulse polarogram for the conversion of 3 into 6. The  $\text{SrCl}_2$  concentrations were (1) 0.00 (2) 0.0685, (3) 0.137, (4) 0.206, (5) 0.27, (6) 0.34 in mM.

of 3. It was thus established for the first time that 1'-sulfo-2'-naphthylazo-6-bromo-2-naphthol forms 1:1 complexes with Ca, Sr, and Ba metal ions in DMF.

Figure 4. Calibration graph for the titration of 3 (0.29 mM) with  $\text{SrCl}_2$  solution in DMF.

**4. Electrochemical Aggregates Determination.** The theoretical equation for the diffusion current obtained with a dropping mercury electrode, which was first derived by Ilkovic, predicts a linear relation between the diffusion current and concentration for a nonaggregating species such as  $\text{Cd}^{2+}$  ions. However, if the pigment is present in aggregates containing  $N$  molecules, the measured diffusion coefficient will be that of the aggregate, i.e., it is expected that  $i/C \neq \text{constant}$ . Therefore, the pigment association number can be obtained via the measurement of the diffusion coefficient.

The relation, which was developed for normal pulse polarography, between the limiting current and the diffusion coefficient of the reduced species is given by the Cottrell equation:<sup>19</sup>

$$i_d^{\text{cath}} = nFAC_R \sqrt{D/\pi t_m} = 2.72 \times 10^5 AC_R \sqrt{D} \quad (2)$$

where  $n$ ,  $F$ ,  $C_R$ ,  $D$ , and  $A$  have their usual meaning and  $t_m$  is the time interval between pulse application and current measurement. This interval is very small (50 ms) in comparison with the drop time of the electrode.

In order to calculate the diffusion coefficient, values of  $A$ ,  $C_R$ , and  $i_d$  had to be determined for each member of the series. The area of the electrode was determined after each experiment according to

$$A = (4\pi)^{1/3} (3mt/d)^{2/3} \quad (3)$$

where  $d$  is the density of mercury ( $13.53 \text{ g/cm}^3$ ). The calculated diffusion coefficient as a function of concentration of the sodium and calcium azo pigment-metal complexes is shown in Tables IV and V.

The relation between the diffusion coefficient and the molecular weight of the molecule is given by the Stokes-Einstein equation:<sup>20</sup>

**Table IV.** The Relation between the Reduction Diffusion Current of Ca NABNS and Concentration

No.	$C_R$ , mmol	$\text{Log } C_R$	$i_d, \mu\text{A}$ N. pulse	$\text{Log } i_d$	$i_d/C$	$D \times 10^6,^a$ $\text{cm}^2 \text{ s}$	$M_{\text{app}}$	$M_n/M_1$
1	0.0476	-4.322	0.370	-0.432	7.90	5.66	495	1
2	0.0788	-4.103	0.60	-0.222	7.60	5.43	557	1.19
3	0.155	-3.81	1.15	0.060	7.42	5.16	701	1.32
4	0.300	-3.523	2.20	0.342	7.33	5.04	856	1.42
5	0.565	-3.248	4.00	0.602	7.08	4.6	654	1.73
6	0.801	-3.096	5.6	0.748	6.99	4.58	921	1.86
7	1.000	-3.00	7.00	0.845	7.00	4.59	921	1.86
8	1.20	-2.92	8.3	0.919	6.90	4.50	985	1.99

$m = 0.904 \text{ mg Hg/s}$ ,  $t = 2.0 \text{ s}$ ,  $m^{2/3}t^{1/6} = 1.05 \text{ mg}^{2/3} \text{ s}^{1/6}$ ,  $A = 0.012 \text{ cm}^2$

<sup>a</sup> The diffusion coefficient calculated using the Cottrell equation  $i_d/C_R = nFA \sqrt{D/\pi t} = 2.72 \times 10^5 AD^{1/2}$ .

**Table V.** The Relation between the Reduction Diffusion Current of Na NABNS and Its Concentration

No.	$C_R$ , mmol	$\text{Log } C_R$	$i_d, \mu\text{A}$	$\text{Log } i_d$	$i_d/C$	$D_2 \times 10^6,$ $\text{cm}^2 \text{ s}^{-1}$	$M_n/M_1$
1	0.0153	-4.815	0.13	-0.886	8.49	5.87	1
2	0.0453	-4.344	0.38	-0.42	8.40	5.72	1.08
3	0.075	-4.125	0.60	-0.222	8.00	5.21	1.43
4	0.148	-3.829	1.16	0.064	7.84	5.00	1.62
5	0.286	-3.544	1.95	0.290	6.82	3.78	3.74
6	0.539	-3.268	3.20	0.505	5.94	2.87	8.58
7	0.763	-3.117	4.10	0.613	5.37	2.35	15.62
8	0.964	-3.016	5.10	0.707	5.29	2.27	17.2
9	1.145	-2.94	5.8	0.763	5.06	2.69	22.4

$m = 0.914 \text{ mg Hg/s}$ ,  $t = 2 \text{ s}$ ,  $m^{2/3}t^{1/6} = 1.057 \text{ mg}^{2/3} \text{ s}^{1/6}$ ,  $A = 0.0128 \text{ cm}^2$

**Table VI.** Spectroscopic Data for Azo Pigment NABNS Metal Complexes in DMF Solution

Metal ion	Na		Mg	Ca		Sr	Ba		
$\lambda_{\text{max}}, \text{cm}^{-1}$	20 200	19 417	20 000	20 290	19 530	20 200	19 490	20 200	19 455
$\epsilon_{\text{max}}, \text{L/mol cm}$ $\times 10^{-4}$	2.43	2.40	1.77	2.07	1.95	2.68	2.61	3.03	2.94

$$D = \frac{2.96 \times 10^{-7}}{\eta} (M/d)^{-1/3} \quad (4)$$

where  $M$  is the molecular weight of the substance and  $d$  its density in the pure solid state, and  $\eta$  is the viscosity coefficient of the solvent. The relation between diffusion coefficient and molecular weights could be used to calculate apparent molecular weights; see Table IV. Alternatively, one can determine the association number of the azo pigment directly from

$$\text{association number} = (M_N/M) = [(i_d/C_R)_0 / (i_d/C_R)_N]^6 \quad (5)$$

where  $(i_d/C_R)_0$  is the ratio of limiting current to concentration in absence of association (i.e., at a very dilute solution). The results indicate that azo pigment **3** (see Table V) starts to aggregate after reaching a concentration of  $5 \times 10^{-5} \text{ M}$  and the aggregation number increases with further increase in pigment concentration, reaching a value of 23 at a concentration of  $1.14 \times 10^{-3} \text{ M}$ . On the other hand, the calcium salt azo pigment starts aggregating at a concentration of  $8 \times 10^{-5} \text{ M}$  and reaches a value of 2 at a concentration of  $1.2 \times 10^{-3} \text{ M}$ . These results are consistent with dimerization with an equilibrium association constant of  $9.5 \times 10^3 \text{ L/mol}$ . The strontium and barium salts also exhibit dimerization but with much smaller association constants,  $2.7 \times 10^3$  and  $2.04 \times 10^3 \text{ L/mol}$ , respectively. The magnesium salt does not show any tendency to dimerize or to aggregate in DMF.

**5. Spectroscopic Aggregate Determination.** The visible absorption spectra of **3-5** are given in Figures 5-7. They exhibit

intense transitions at  $\sim 20\,200$  and  $\sim 19\,450 \text{ cm}^{-1}$ , for which the molar extinction coefficients are given in Table VI.

Pigments **5** and **7** are the only ones that exhibit an isosbestic point, at  $21\,980$  and  $21\,280 \text{ cm}^{-1}$ , respectively. Interestingly, successive increases in concentration of pigments **5** or **7** result in a red shift of the absorption peaks and a substantial increase in the apparent extinction coefficient, which is opposite to dimerization of azo dyes where a blue shift and decrease in  $\epsilon$  is usually observed. Both pigments **3** and **4** shows no concentration-dependent spectra within experimental uncertainty. On the other hand, with pigment **6** (Sr) a decrease in the apparent  $\epsilon$  with increase of concentration was observed.

From the concentration-dependent spectra of **5** (Ca), the calculation of the pure monomer spectrum, pure dimer spectrum, and equilibrium constant is accomplished using a computer best fit program.<sup>21</sup> In the analysis it is assumed that the monomer concentration,  $C_m$ , and dimer concentration,  $C_d$ , follow the law of mass action:

$$K_{\text{eq}} = C_d/C_m^2 \quad (6)$$

where  $K_{\text{eq}}$  is the association constant for the dimer formation. If the total pigment concentration,  $C_t$ , is small so that no higher aggregates are formed, then

$$C_d = (C_t - C_m)/2 \quad (7)$$

Assuming that eq 6 and 7 are valid, a best-fit monomer and dimer spectrum can be calculated for a given  $K_{\text{eq}}$ . By varying  $K_{\text{eq}}$  systematically, the best-fit values of  $\epsilon_m$ ,  $\epsilon_d$ , and  $K_{\text{eq}}$  are found where  $\epsilon_m$  and  $\epsilon_d$  are the molar extinction coefficients of

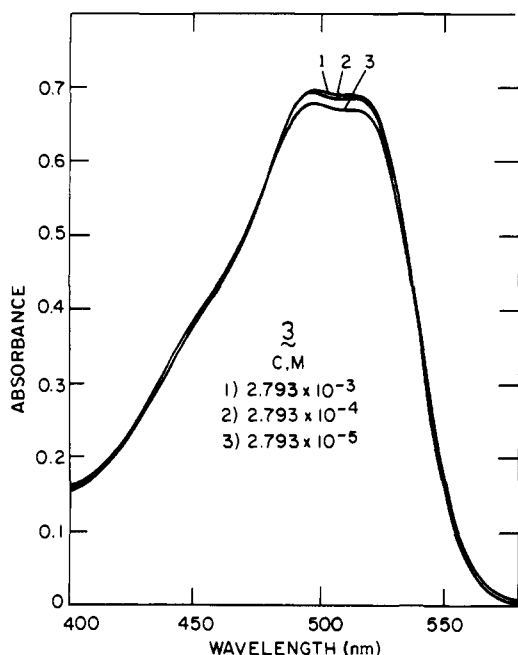


Figure 5. Visible absorption spectra of **3** as a function of concentration in DMF.

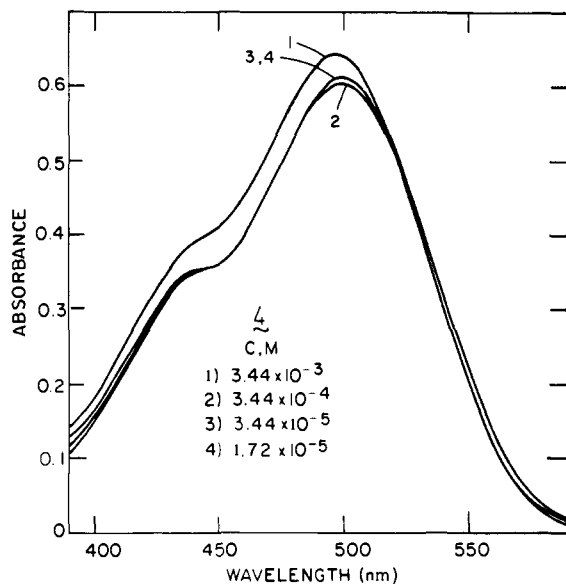


Figure 6. Visible absorption spectra of **4** in DMF as a function of concentration.

monomer and dimer, respectively. The best-fit  $\epsilon_m$  and  $\epsilon_d$  are then used to calculate  $K_{eq}$  and its error at each concentration. The result of this calculation is shown in Figure 8 for **5**. The solid line is drawn with a theoretical slope of 2.00, as predicted by eq 7. The best-fit monomer and dimer spectra are shown in Figure 9. The calculated  $K_{eq}$  from the spectroscopic technique was  $(9.09 \pm 0.5) \times 10^3$  L/mol, which is in excellent agreement with that obtained from polarographic measurements.

Attempts were made to analyze the spectra of pigment **6** and **7**; however, no best fit of the data was obtained, since the changes in optical absorption over the concentration range used were very small. As we have described earlier, both **6** and **7** exhibit aggregation in DMF which was detected by polarography but not by the spectroscopic technique.

## Discussion

### 1. Polarography of the Sodium Salts of NABN Sulfonate, **3**. The polarographic reduction of the sodium salt, **3**, in DMF

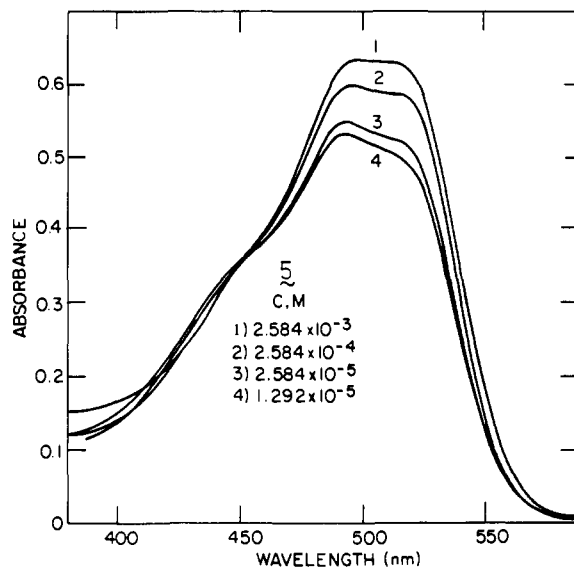
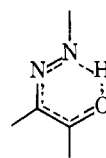


Figure 7. The concentration-dependent visible absorption spectra of **5** in DMF.

solution was found to be quite similar to those of arylazo-2-naphthols<sup>1</sup> in aprotic solvents. The first reduction wave ( $E_{1/2} = -1.09$  V vs. SCE) represents a reversible one-electron transfer to form the corresponding radical anion. The second reduction wave ( $E_{1/2} = -1.4$  V) is most reasonably explained as a reversible one-electron transfer followed by a fast chemical reaction, probably a protonation step. A third reduction wave ( $E_{1/2} = -1.69$  V) was also observed which may represent the reduction of the chemical product. The relative height of the second and third waves was found, as expected, to be dependent on the scan rate.

Comparing the first half-wave reduction of **3** with that of 2,2'-azonaphthalene<sup>17</sup> indicates a 130-mV anodic shift due to the attachment of the *o*-hydroxy group, neglecting the influence of the bromo and sulfonic acid groups. This is consistent with results of Meche and Schmal,<sup>22</sup> where the  $E_{1/2}$  of *p*-hydroxy azo dyes were found to be 100 mV more positive than those of the corresponding azo dye. This was explained in terms of internal hydrogen bond formation, i.e.,



### 2. Influence of Metal Ions on the Polarographic Reduction of **3**.

Despite the extensive literature on the electrochemistry of azo compound metal complexes in aqueous and other protolytic solvents, almost no studies have been carried out on the electrochemical behavior of these complexes in aprotic media. The addition of alkaline earth metal chloride solution in DMF to that of **3** resulted in every case in a split of the first reduction wave into two. The height and the reduction potential of the second wave was found to be dependent on the amount and nature of the metal ion, respectively. It is thus possible to classify the azo pigment **3** as a polarographically active pigment in DMF solution. In contrast to the results in protolytic solvents, where a two-electron reduction of the azo to the hydrazo compound is observed, the reduction of azo-metal complexes in DMF proceeds via two one-electron steps. In addition, the magnitude of reduction wave displacement for **3** in DMF was found to be three times as large as the typical 60-100-mV shift observed in protolytic solvents for Mordant dyes. Present evidence indicates that in the case of azo pigment **3** the hydroxy and sulfonic groups can get close enough to

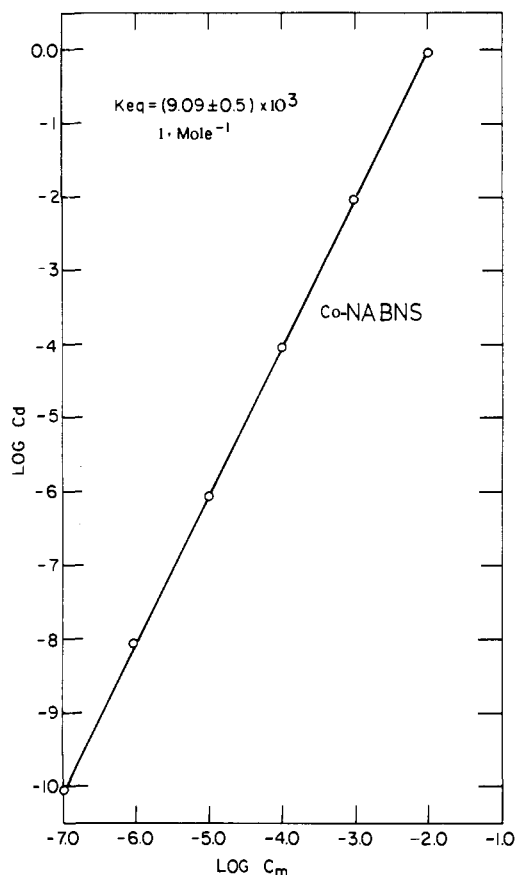


Figure 8. Plot of  $\log C_d$  vs.  $\log C_m$  for azo pigment **5** in DMF, solid line drawn with the overall slope of two.

gether to bond with the metal ion to form two adjacent, six-membered ring systems having partial bond formation between the azo nitrogen and the metal ion. The stability of the complexes was found to vary in the order  $\text{Ca}^{2+} > \text{Sr}^{2+} > \text{Ba}^{2+}$ . Similarly, the stable Ca complex, **5**, exhibited the largest anodic shift of the reduction wave:

complexed metal ion	$\text{Ca}^{2+}$	$\text{Sr}^{2+}$	$\text{Ba}^{2+}$
$\Delta E_{1/2}$ , mV	300	210	180
$-E^{\text{red}}$ ( $\text{M}^{2+} + 2e \rightleftharpoons \text{M}$ )	2.87	2.89	2.90

The magnitude of the observed shifts correlates linearly with the electronegativity of the metal ion and with the equilibrium association constant, as shown in Figure 10, with the exception of magnesium. These results are consistent with those of Snavely et al.<sup>23</sup> where the stability constant of a number of 1-(2-hydroxyphenylazo)-2-naphthol complexes with bivalent ions appears to be  $\text{Zn}^{2+} > \text{Cd}^{2+} > \text{Mg}^{2+} > \text{Ca}^{2+} > \text{Sr}^{2+} > \text{Ba}^{2+}$ . The only exception which we found is with the magnesium complex. The anomalous behavior of the magnesium complex will be discussed later. The potentiometric titration measurements indicated that alkaline earth metal ions chemically react with **3** to produce the complex which is reduced at a more positive potential. The ratio of metal ion to azo pigment in the final product in all cases was found to be 1:1, since the limiting reduction current of **3** reached zero at a metal ion concentration equivalent to the initial concentration of **3**. A simple chemical reaction scheme is consistent with these observations (see Scheme I).

At low concentration of alkaline earth metal ions with respect to that of azo pigment, **3**, the formation of a complex where the metal ion reacts with two pigment molecules cannot be excluded. The reduction potential of these materials is expected to be quite similar to that of **3**, since the environment around the azo chromophore stays the same. However, at

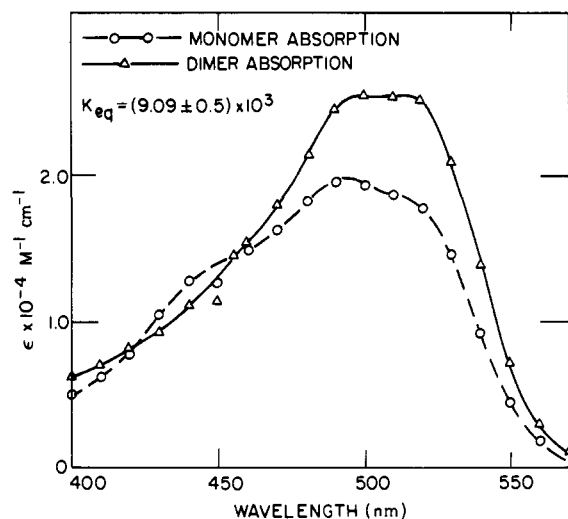


Figure 9. Calculated absorption spectra of pure monomer and dimer of azo pigment **5** in DMF.

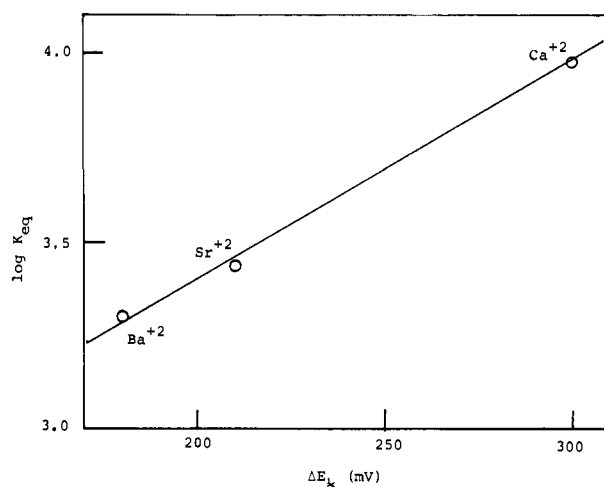
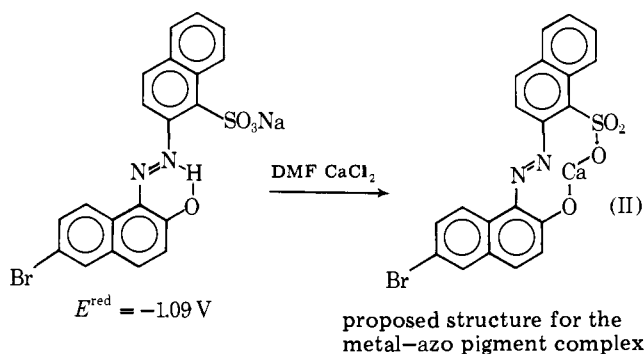


Figure 10. The relation between the association equilibrium constant and the magnitude of reduction shift.

Scheme I



higher metal ion concentrations, the 1:1 azo pigment-metal complex will be formed. The structure is probably a strain-free six-membered ring (II). A similar structure was proposed for the chromium'-o,o'-dihydroxy azo dye.<sup>24</sup>

**3. Dimerization and Aggregation.** The solid state properties of azo pigments, such as optical characteristics and photoactivity, are certainly related to the molecular structure of the material. Therefore, an understanding of the interaction between pigment molecules is of importance, since it could provide clues to the origin of photoactivity and can explain the observed optical properties of the solid material. Aggregation

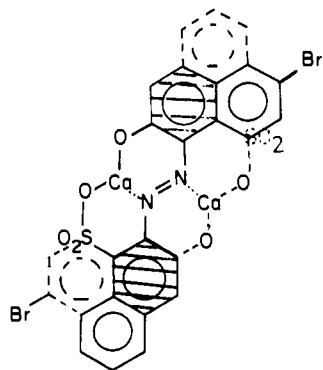


Figure 11. Proposed structure for *o'*, sulfonic, *o*-hydroxy azo pigment-calcium complex dimer (shaded area indicates the overlapping of the two rings; the two Br and SO<sub>3</sub> groups are as far apart as possible).

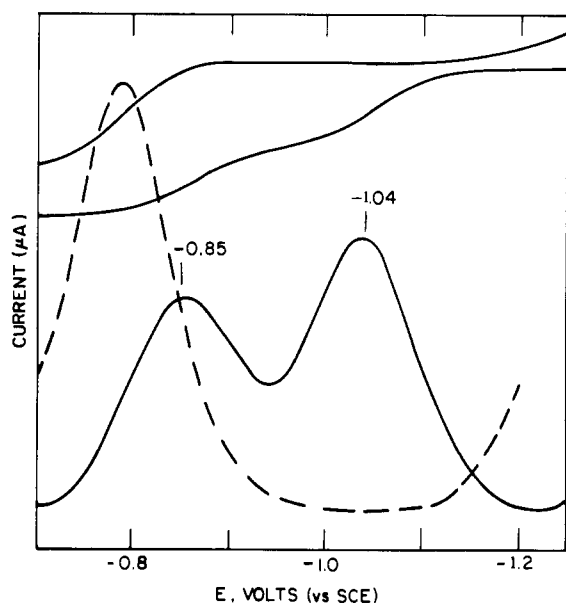


Figure 12. Polarographic reduction of azo pigment **8** in DMF (—), and after addition of excess CaCl<sub>2</sub> solution (- - -).

and dimerization of azo dyes has been extensively studied in aqueous solution through a number of experimental approaches. However, owing to the insolubility of azo pigments and their metal complexes in most common solvents, there have been no reported studies of molecular aggregation of these materials. We found dimethylformamide to be an excellent solvent for most azo pigments and their metal complexes up to ca.  $>10^{-2}$  M.

The relation between the limiting current and concentration of the sodium azo pigment **3** indicated that this pigment starts to associate at a concentration of  $5 \times 10^{-5}$  in DMF. The average aggregation number reached two (dimer) at a concentration of  $2.5 \times 10^{-4}$  M (see Table V), with an apparent equilibrium constant of  $1.5 \times 10^4$  L/mol. However, the aggregation number increased rapidly with a further increase in pigment concentration, reaching a value of 23 at a concentration of  $1.14 \times 10^{-3}$  M. These results are consistent with linear aggregation via hydrogen bonding. It is expected and was found that this type of aggregation resulted in a very small, if any, spectral change, since the delocalized electrons in the pigment molecules do not participate in the aggregation process (see Figure 5).

On the other hand, the azo pigment-calcium complex, **5**, starts aggregating at a concentration of  $8 \times 10^{-5}$  M and reaches a value of two at a concentration of  $1.2 \times 10^{-3}$  M. The polarographic and spectroscopic results are consistent with

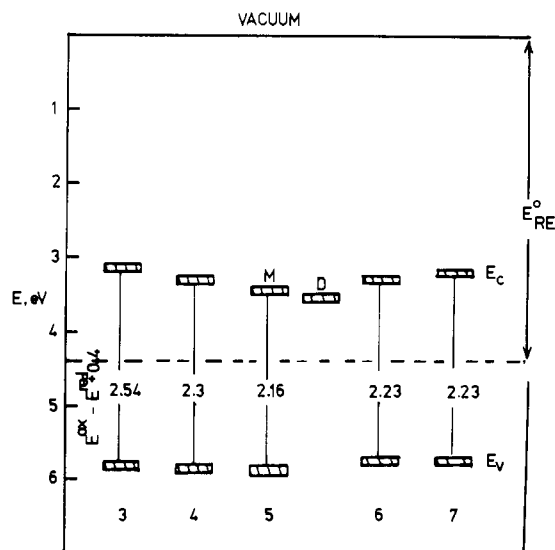


Figure 13. Energy level diagram of the valence and conduction levels of azo pigment metal complexes.

Table VII. Calculated and Experimental Diffusion Coefficients of Azo Pigment NABNS Metal Complexes

No.	Metal ion	$D_{\text{obsd}} \times 10^6$ , cm <sup>2</sup> /s	$D_{\text{calcd}} \times 10^6$ , <sup>a</sup> cm <sup>2</sup> /s
3	Na	5.87	5.73
4	Mg	4.50	5.71 (4.54)
5	Ca	5.66	5.66
6	Sr	5.05	5.49
7	Ba	5.22	5.30

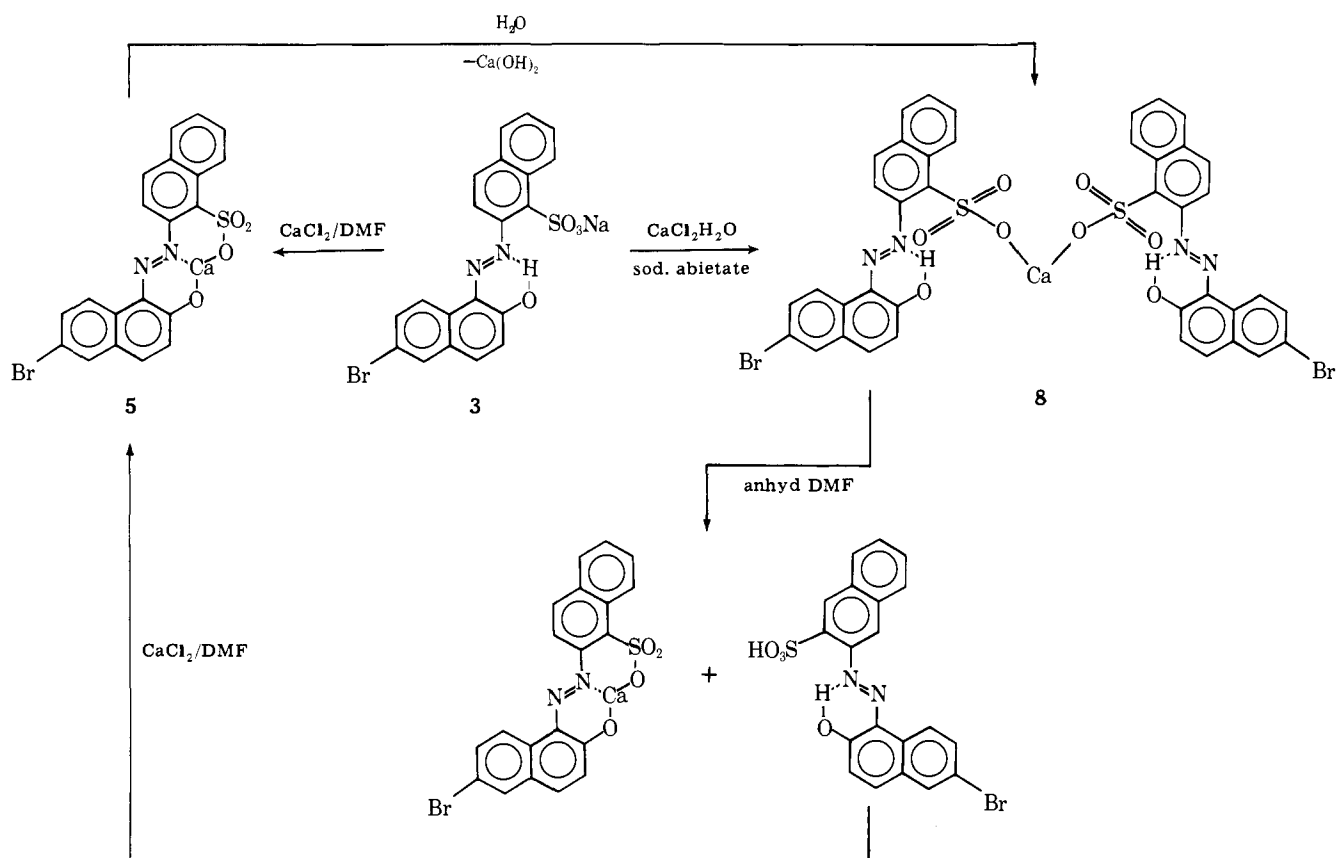
<sup>a</sup> The density of the pure solid was estimated to be 1.7 g/cm<sup>3</sup>. The value in bracket is the calculated diffusion coefficient for the structure (azo pigment)<sub>2</sub>:Mg<sup>2+</sup>.

dimerization with an association constant of  $9.5 \pm 0.5 \times 10^3$  L/mol. The absorption spectrum of the pure dimer (Figure 9) is red shifted from that of the monomer. In addition, the dimer has a higher extinction coefficient. This suggests that the delocalized electrons in the pigment molecules are participating in the formation of the dimer, which is in accord with a parallel plane dimerization. A proposed structure of the dimer is given in Figure 11. Evidence for the participation of the azo group in the dimerization process is the observed anodic shift of the reduction potential of **5** by about 50 mV on dimerization.

Similarly, the strontium and barium metal complexes exhibited some tendency for dimerization in DMF; however, the association constant is a factor of 5 less than that for the calcium complex. Apparently the association equilibrium constant increases with the increase of the reduction wave shift (see Figure 10) with the exception of the magnesium complex which does not associate in DMF solution.

**4. Polarographic Analysis of Azo Pigment 8.** The polarographic behavior of pigment **8** showed two reduction waves; see Figure 12. A reduction wave at  $-0.85$  V which is similar to the intramolecularly complexed calcium salt of the pigment, and the second reduction wave at  $-1.03$  V which is similar to that of metal-free pigment. This mixture, when treated with 0.5 mol of CaCl<sub>2</sub>, resulted in the disappearance of the second reduction wave and a doubling of the limiting current of the first wave; see Figure 12. From these results it is reasonable to assume that pigment **8** (1:2) disproportionates in DMF solution to the more soluble intramolecularly complexed calcium salt and metal-free azo pigment molecules. This is unfortunate, since it did not allow us to examine directly the molecular properties of pigment **8**.

Scheme II



It is worth noting that attempts to isolate the intramolecularly complexed calcium salt of NABNS sulfonate, **5**, via aqueous precipitation resulted in its hydrolysis and conversion to **8**, as shown in Scheme II. The intramolecularly complexed azo pigment **5** was successfully isolated from a DMF solution of **8** by adding an equivalent quantity of  $\text{CaCl}_2$  by benzene.

**5. The Absolute Energy Levels of Azo Pigment NABNS-Metal Complexes. a. The Relation between Gas Phase and Solution Ionization Potentials and Electron Affinities.** The half-wave oxidation potentials of various azo pigment NABNS-metal complexes were determined voltammetrically in DMF solution (see Table III). These are related to the gas phase ionization energy,  $I_g$ , according to<sup>25</sup>

$$E_{1/2}^{\text{ox}} = I_g - \Delta E_{\text{solv}} - E_{\text{RE}}^0 \quad (8)$$

where  $E_{\text{RE}}^0$  is the free energy of the electron in the SCE reference electrode (4.38 eV).  $\Delta E_{\text{solv}}$  is the differential real solvation energy of the radical cation, usually taken to be the difference between the electrostatic energy of the ion in solution and that in vacuo. This term can be calculated using the familiar Born relation

$$\Delta E_{\text{solv}} = \frac{e^2}{2r} \left( 1 - \frac{1}{\epsilon_s} \right) \quad (9)$$

where  $r$  is the radius of the ion and  $\epsilon_s$  is the bulk dielectric constant of the solvent ( $\epsilon_{\text{DMF}} = 36.7$ ). The value of  $\Delta E_{\text{solv}}$  for large organic radical anions or cations is usually constant and equals 2.0 eV.<sup>26</sup> Similarly, the half-wave reduction potential of these materials is related to the gas phase electron affinity,  $\text{EA}_g$ , according to

$$E_{1/2}^{\text{red}} = \text{EA}_g + \Delta E_{\text{solv}} - E_{\text{RE}}^0 \quad (10)$$

**b. The Relation between Solid State and Solution Ionization Potentials and Electron Affinities.** In condensed media (solid

state) the ionization potential  $I_c$  is reduced from that required under vacuum by an amount equivalent to the crystal polarization energy,  $P_c$  [ $P_c = e^2/2r(1 - 1/n^2)$ ], where  $r$  is the average radii of the charged product and  $n$  is the refractive index. Thus,

$$I_c = I_g - \frac{e^2}{2r} \left( 1 - \frac{1}{n^2} \right) \quad (11)$$

Similarly, the solid state electron affinity is greater than that in vacuum by the crystal polarization energy, i.e.,

$$\text{EA}_c = \text{EA}_g + \frac{e^2}{2r} \left( 1 - \frac{1}{n^2} \right) \quad (12)$$

For the azo pigments discussed here, where  $n = 3.2$  and  $r = 3.4 \text{ \AA}$ , the value of  $P_c$  is approximately 1.80 eV.<sup>27</sup> Combining eq 8 and 11,

$$I_c = E_{1/2}^{\text{ox}} + E_{\text{RE}}^0 - P_c + \Delta E_{\text{solv}} \quad (13)$$

Similarly, from eq 10 and 12,

$$\text{EA}_c = E_{1/2}^{\text{red}} + E_{\text{RE}}^0 + P_c - \Delta E_{\text{solv}} \quad (14)$$

Taking the value of  $\Delta E_{\text{solv}}$  as 2.0 eV and that of  $P_c$  as 1.80 eV, it is possible to construct an energy level diagram for this series of azo pigment metal complexes as shown in Figure 13. It is obvious that **5** in the solid state has the lowest energy gap (2.16 eV).

#### 6. Anomalous Behavior of the Magnesium NABNS Sulfonate

**4.** The addition of magnesium chloride to the sodium salt, **3**, solution in DMF results in a small anodic shift of the polarographic reduction wave. This is in contrast to Snaveley's<sup>23</sup> results, where magnesium forms a stable five-membered ring complex with *o,o'*-dihydroxy diarylazo dyes. Furthermore, the displaced wave appears as a composite of two reduction steps; see Figure 1c. This abnormal behavior of the magnesium salt

was also reflected in its visible absorption spectrum, which exhibits a single band at 500 nm in DMF. Most interestingly, no tendency toward dimerization or aggregation was observed, and this suggests a different molecular structure for the magnesium complex. Magnesium ion analysis of the isolated solid pigment using atomic absorption indicated the presence of 3.2% magnesium. This indicates that the material exists predominantly in the 1:2 structure.

It is quite possible that the water of hydration was not totally removed from the magnesium chloride salt and prevented the formation of two six-membered ring system as shown for structure II in Scheme I. Instead, the magnesium intermolecularly binds two pigment molecules.

A comparison of the experimentally determined diffusion coefficient,  $D$ , of the various azo pigment-metal complexes with that calculated from the Stokes-Einstein equation is given in Table VII. The agreement is generally good with the exception of the magnesium complex, where the observed diffusion coefficient is much less than that calculated for the intramolecular complex. However, the calculated  $D$  for the structure (azo pigment)<sub>2</sub>:Mg<sup>2+</sup> is in excellent agreement with the observed value, which supports the validity of the proposed structures.

### Conclusion

The polarographic technique was utilized not only to determine the absolute energy levels of molecules in solution, but also to provide insight into the azo pigment-metal ion complex formation, and subsequent molecular association in non-aqueous media.

The sodium salt of azo pigment **3** showed a tendency toward the formation of high molecular weight aggregates. This aggregation occurs in plane via hydrogen bonding without the participation of the delocalized electrons of the azo molecules. This is generally true for sodium sulfoaryloazo-2-naphthols. However, the calcium salt of the azo pigment exhibited a

definite tendency toward dimerization in DMF. The visible absorption spectrum of the dimer was found to be shifted to the red and has a higher extinction coefficient than that of the monomer. These results indicate that the delocalized electrons of the azo molecules are involved in the dimerization, i.e., the dimer has a parallel plane structure.

### References and Notes

- (1) J. R. Kuder, P. J. Cressman, F. D. Saeva, D. Wychick, and G. C. Hartmann, *J. Chem. Phys.*, **61**, 2740 (1974).
- (2) E. Rabinowitch and L. F. Epstein, *J. Am. Chem. Soc.*, **63**, 69 (1941).
- (3) W. C. Holmes and R. Standing, *Trans. Faraday Soc.*, **41**, 542, 568 (1945).
- (4) P. Alexander and K. A. Stacey, *Proc. R. Soc. London, Ser. A*, **212**, 274 (1952).
- (5) E. I. Valko, *J. Am. Chem. Soc.*, **63**, 1433 (1941).
- (6) R. B. McKay and P. J. Hillson, *Trans. Faraday Soc.*, **61**, 374 (1965).
- (7) T. Vickerstaff, "The Physical Chemistry of Dyeing", 2nd ed. Oliver and Boyd, London, 1954, Chapter 3.
- (8) I. D. Rattee and M. M. Brener, "The Physical Chemistry of Dye Adsorption", Academic Press, New York, N.Y., 1974, Chapter 4.
- (9) E. Coates, *J. Soc. Dyers Colour.*, **85**, 355 (1969).
- (10) F. D. Saeva, *J. Org. Chem.*, **36**, 3842 (1971).
- (11) J. E. Kuder, *Tetrahedron*, **28**, i973 (1972).
- (12) A. R. Monahan and J. B. Flannery, Jr., *Chem. Phys. Lett.*, **17**, 510 (1972).
- (13) F. G. Thomas and K. G. Boto, "The Chemistry of the Hydrate, Azo and Azoxy Groups", S. Patai, Ed., Wiley, New York, N.Y., 1975, Chapter 12.
- (14) G. W. Latimer Jr., *Talanta*, **15**, 1 (1968), and references cited therein.
- (15) A. G. Fogg, J. L. Kumar, and D. T. Burns, *Analyst*, **94**, 262 (1969); **96**, 403 (1971).
- (16) T. M. Florence, *J. Electroanal. Chem. Interfacial Electrochem.*, **50**, 113 (1974); **53**, 115 (1974).
- (17) A. Bard and J. L. Sadler, *J. Am. Chem. Soc.*, **90**, 1979 (1968).
- (18) M. M. Willard and J. A. Dean, *Anal. Chem.*, **22**, 1264 (1950).
- (19) K. B. Oldham and E. P. Parry, *Anal. Chem.*, **42**, 000 (1970).
- (20) I. M. Kolthoff and J. J. Lingane, *Polarography*, **1**, 56 (1952).
- (21) The author is indebted to Mr. L. Marks for valuable help in writing and adapting the computer program to the XRCR terminal system.
- (22) T. Iijima and M. Sekido, *J. Soc. Dyers Colour.*, **76**, 354 (1965).
- (23) F. A. Snavely, W. C. Eirnelius, and B. E. Douglas, *J. Soc. Dyers Colour.*, **73**, 491 (1957).
- (24) G. Schetty, *J. Soc. Dyers Colour.*, **71**, 705 (1955).
- (25) R. O. Loutfy, *J. Chem. Phys.*, in press.
- (26) V. D. Parker, *J. Am. Chem. Soc.*, **98**, 98 (1976).
- (27) H. Meier, *Monogr. Mod. Chem.*, **2**, 423 (1974).

## Substituted Benzocyclobutenes, Indans, and Tetralins via Cobalt-Catalyzed Cooligomerization of $\alpha,\omega$ -Dienes with Substituted Acetylenes. Formation and Synthetic Utility of Trimethylsilylated Benzocycloalkenes<sup>1</sup>

R. L. Hillard III and K. Peter C. Vollhardt\*<sup>2</sup>

Contribution from the Department of Chemistry, University of California, Berkeley, and the Materials and Molecular Research Division, Lawrence Berkeley Laboratory, Berkeley, California 94720. Received September 13, 1976

**Abstract:** A new synthesis of substituted benzocyclobutenes, indans, tetralins and two model anthraquinones is described which utilizes the catalytic ability of  $\eta^5$ -cyclopentadienyldicarbonylcobalt to cooligomerize  $\alpha,\omega$ -dienes with substituted monoacetylenes. Yields are best when bis(trimethylsilyl)acetylene (BTMSA) is used as one of the reactants to give the ortho-bis(trimethylsilyl)ated derivatives **8a**, **14a-16a**, and **18a**. Reaction of monosubstituted dienes with unsymmetrical monoacetylenes yields the sterically more hindered aromatic products **8d** and **8f**. Catalytically inert cyclobutadiene cyclopentadienyl cobalt complexes are formed in side reactions when BTMSA is cooligomerized with  $\alpha,\omega$ -dienes. These include complexes derived from reaction of one (**19**) or both (**20**, **21**) ends of the diene molecule. The synthetic utility of the *o*-bis(trimethylsilyl)benzene unit in electrophilic substitutions is demonstrated. Selective and stepwise displacement of the trimethylsilyl groups by electrophiles results in a variety of new derivatized benzocycloalkenes. Some mechanistic considerations are presented.

Cyclization reactions comprise an important class of synthetic transformations at the disposal of the organic chemist. In the majority of cases these reactions lead to saturated or

partially unsaturated five- or six-membered rings, whereas benzene rings are formed only on rare occasions. Synthetic strategy to complex molecules of interest containing benzene